WELDED JOINTS OF RECTANGULAR HOLLOW SECTION MADE OF HIGH STRENGTH STEEL (HSS)

Haohui Xin[1*], Prishilla Kisoensingh[1], and Milan Veljkovic[1]

[1]*Faculty of Civil Engineering & Geosciences, Delft University of Technology, 2628 CD Delft, Netherlands*
E-mail: H.Xin@tudelft.nl

A new draft version of Eurocode 3 part 1-8 provides design equations for rectangular hollow section (RHS) joints up to S700. In this paper, finite element simulations of gap K-joints are conducted to investigate effects of material properties, gap size of the joint, the brace to chord width ratio (β) and welds type on the secondary bending stresses and the resistance. The governing failure mode considered for all the FE models is the chord face failure followed by brace sidewall failure. The ratio of axial stresses over the nominal stress was lower in the compressive brace of the joints with higher strength steel grades compared to the mild-strength joints. The maximum secondary bending stresses varied between 0.12fy and 0.32fy. The secondary bending stresses are increasing with the increase of the steel grade and β-value, and with reducing the gap size. The level of secondary bending stresses varied between 38% and 56% of the average normal axial stress. Compared to the butt-welded joints, larger secondary bending stresses were obtained in the fillet-welded joints. The yield line model is used to predict the ultimate load and good agreement is obtained compared with FE results.

Keywords: Rectangular hollow section (RHS) joints; High-strength steels; Ultimate load; Secondary bending stress.

1 INTRODUCTION

The interest in high strength steel (HSS) with yield strength above 460 MPa shows an increasing trend, mainly due to its high yield strength, low weight to strength ratio. The HSS has the potential for applications in specific structures, such as in truss girders of long spans used in sports arenas and bridges (Veljkovic & Johansson 2004, Bijlaard et al. 2019). One obstacle for competitive use in engineering practice is due to uncertainties in whether current design standards of RHS joints validated for mild-strength steels up to S460 can be applied to HSSs. An open question on what would be justified level of material factors necessary to accept.

Secondary bending stresses in tubular joints appear due to the non-uniform stiffness of the joint, eccentric forces and the large deformations in a truss girder. The calculation of the secondary bending stresses is complex because it does not only depend on the joint stiffness but also on the behavior of the joint. To simplify the strength calculation, truss girders are designed using pinned jointed braces and continuous chords (Wardenier et al. 2002). The European design code (EN1993-1-8:2005) which is applicable to welded hollow section joints with steel grade up to S460 neglects the secondary bending stresses for joints within the validity. A new version of European standard part 1-8 chapter 9, still under discussion at the time of writing of this paper (EN1993-1-8-DRAFT V4.2, 2018), proposes design rules for RHS joints with a yield strength up to 700MPa. The design rules, which were originally developed by CIDECT, are based on

Proceedings of the 17th International Symposium on Tubular Structures.
Editors: X.D. Qian and Y.S. Choo

Published by Research Publishing, Singapore.
ISBN: 978-981-11-0745-0; doi:10.3850/978-981-11-0745-0_068-cd

experimental, numerical and analytical analysis and validated for a range of parameters for steel grades up to S460. The validity range gives various limitations on geometrical parameters of joints to ensure that the members and the joints have sufficient resistance validated by the design resistance formulae.

Bjork et al. 2015 showed that the secondary bending moment is highly dependent on the joint geometry and material properties. Their results showed that the secondary bending stresses requires additional attention if high strength steels are used. The secondary bending moment is dependent on the plastic moment capacity of the brace member or the joints. The trilinear stress-strain relationship without softening or damage in their finite element simulation may lead to an unreal increase of secondary bending moment especially when the local material is in the stage of the post necking or fracture.

The impact of HSS on the behavior of hollow section joint may be different and must be therefore checked. In this paper an attempt is made to investigate the effect of the secondary bending stresses for four steel grades, two gap size, three braces to chord width ratios (β) and two types of welds. A parametric study is performed on an individual gap K-joint made of square hollow sections. The influence of the material properties, gap size, the brace to chord width ratio and weld type on the RHS joints with respect to the secondary bending stresses and the failure modes is the primary goal of the analysis.

2 FINITE ELEMENT MODEL

The parameter symbols for the gap K-joint are shown in Fig.1 and the considered values are summarized in Table 1. The length of each member is set to 5 times the member's width, b_i to ensure that the stresses at the joint zone are not influenced by the boundary conditions. Both brace members are made with the same cross-section and have the same inclination, θ_i=30^0. The parameter β is the brace width to chord width ratio. Four material properties of S355, S460, S700, S960, two gap size of G_0=25mm and G_1=40mm, three braces to chord width ratios of β_1=0.50, β_2=0.57 and β_3=0.67, fillet and butt welds are varied to investigate their effects on the secondary bending stresses and the failure modes. The weld width t_w of fillet welds is dependent on the brace thickness and the yield strength of the material, as listed in Table 2. A "numerical" gap of 0.15mm between the chord and brace members is considered in the analyses. The stress-strain curves for the steel grade varying from S355 to S960 are taken from RUOSTE (2016) project. It should be noted that ratio of yield strength to tensile strength is 0.75 for S355, 0.80 for S460, 0.84 for S700, and 0.82 for S960, based on results from RUOSTE (2016) project.

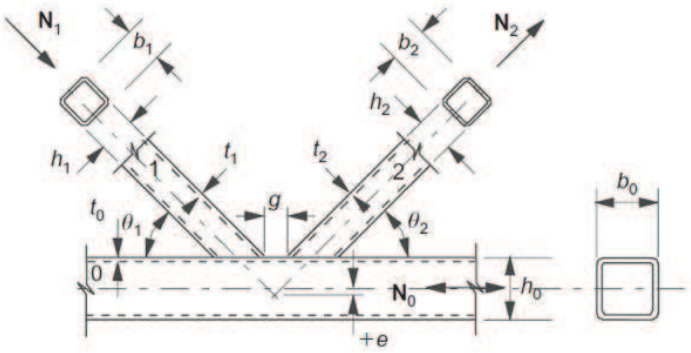

Figure 1. Gap K-joint parameters

Table 1. Joint geometry for the parametric study

Joint layout	b_o	t_o	b_i	t_i	g	θ_i	e	β	Weld
	(mm)	(mm)	(mm)	(mm)	(mm)	(°)	(mm)	(-)	
K1	120	5	80	5	40	30	-2.3	0.67	Fillet
K2	120	5	80	5	25	30	-6.6	0.67	Fillet
K3	140	6.3	70	5	40	30	-18	0.50	Fillet
K4	140	6.3	80	5	40	30	-12.3	0.57	Fillet
K5	140	6.3	90	5	40	30	-5.5	0.67	Fillet
K6	140	6.3	70	5	40	30	-18	0.50	Butt
K7	140	6.3	80	5	40	30	-12.3	0.57	Butt
K8	140	6.3	90	5	40	30	-6.5	0.53	Butt

Table 2. The weld width, t_w, used in FEA

Steel grade	Weld size	
$f_y \leq 500$ MPa	$t_w \geq 1.4t_i$	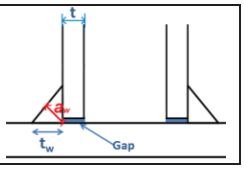
500 MPa < f_y < 700 MPa	$t_w \geq 1.69t_i$	
700 MPa < $f_y \leq 960$ MPa	$t_w \geq 1.98t_i$	

3 FINITE ELEMENT MODEL

3.1 Stress distribution at deformation limit

The stress distribution at 3%b_o deformation limit in the FE models is shown in Fig. 2. The governing failure mode for all the FE models is the chord face failure. In the zone of welds, the stresses can be higher than the nominal yield strength. For the models G1-S355 and G1-S460 the stresses are approximately 55% and 44% larger. In high strength joints this level is 27%. Compared to the joints with mild strength steel, lower stresses to yield strength ratio appear in the high-strength joints.

3.2 Effects of the material properties

Fig. 3 shows the load-displacement relationship of K1 joints with different steel grades. Note that N_R is the design resistance without considering the material factor (C_f) and the partial safety factor, and $N_{R,CF}$ is the design resistance only considering the material factor (C_f) based on the proposed new version of European standard part 1-8 chapter 9. The load corresponding to the 3%b_0 deformation limit is considered as the ultimate of the joints. Obviously, joints with higher yield strength will result in higher ultimate capacity. Joints with steel grade S460, S700, and S960 resulted in 20%, 83% and 142% larger resistance compared to joint with steel grade S355. The ratio of secondary bending stress to the yield strength (σ_m/f_y) is also plotted against the ratio of the average axial stress to the yield strength (σ_n/f_y) in Fig. 4. For the K joints with S355 and S460 steel grades, the largest secondary bending moment is $0.22f_y$. For K joints with S700 and S960, the secondary bending moment is 23% and 30% respectively, larger than the models with mild-strength steels. At ultimate load resistance, the average stresses for joints with HSS vary from $0.73f_y$ to $0.75f_y$ and the secondary bending stresses from $0.04f_y$ to $0.06f_y$ respectively.

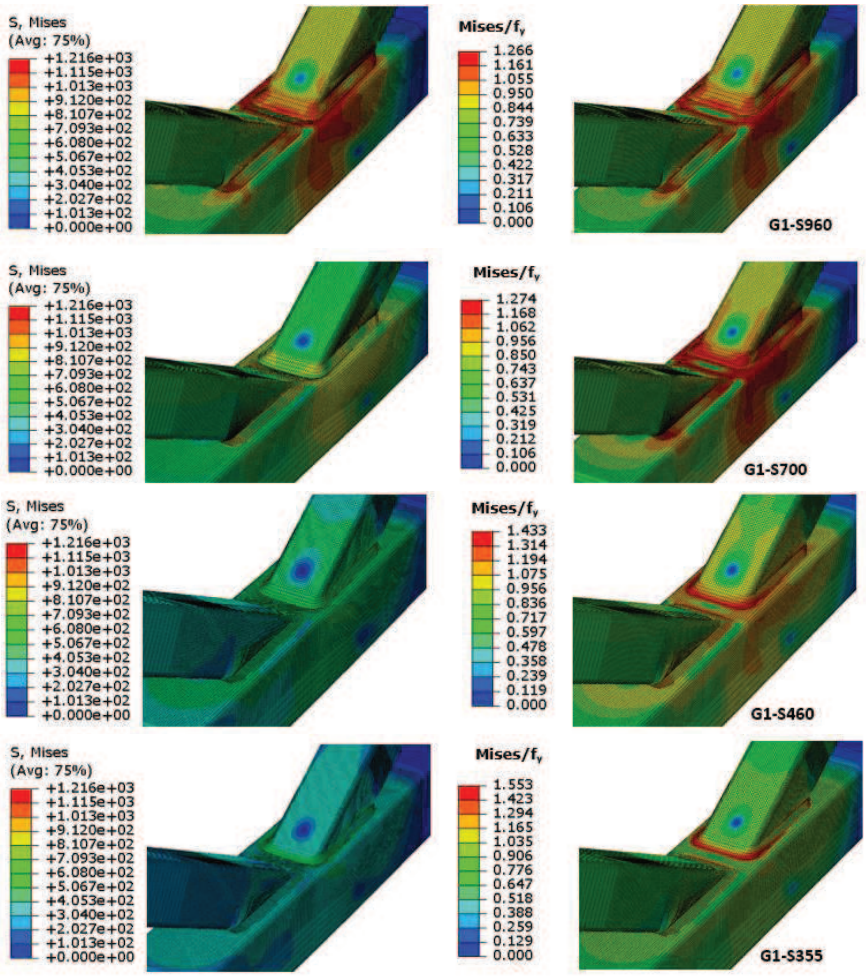

Figure 2. Mises stresses distribution of K-gap joints

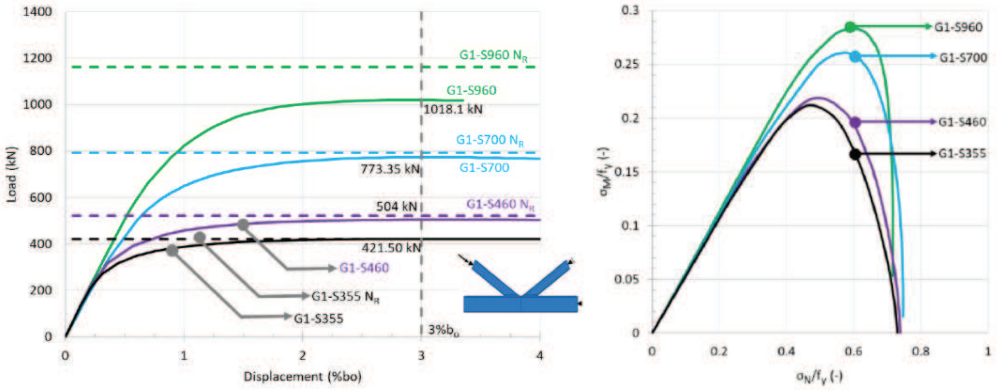

(a) (b)

Figure 3 Material properties effects (a) Load-displacement (b) The secondary bending stress

3.3 Effects of the gap size

A selection of load-displacement curves and secondary bending stress with different gap sizes are shown in Fig. 4, note that the points in Fig.4-b corresponds to the ultimate force. The joints with lower gap sizes have larger stiffness leading to higher resistance. The ultimate load resistance for the FE model G1-S355 is 421 kN, and for G0-S355 is 445 kN. The model with the lower gap size, G0-S355 result in 6% larger ultimate load resistance than the model G1-S355. This percentage is also 6% for S460, 9% for S700 and 12% for S960. For each steel grade, the secondary bending stresses with smaller gap size are higher than that of the models with larger gap size. Comparing both the gap sizes, the FE models with the smaller gap size result in 7%-15% larger secondary bending moment. The largest percentage is obtained for joints with HSS and the lowest for joints with S355.

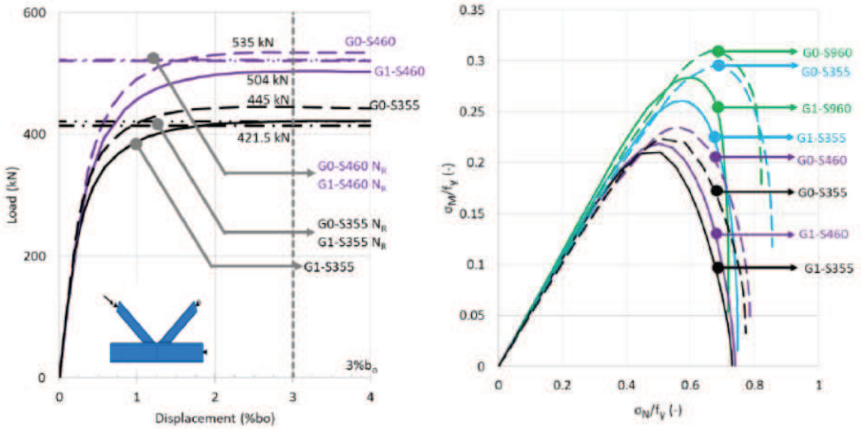

(a) (b)

Figure 4 Gap size effects (a) Load-displacement (b) The secondary bending stress

3.4 Effects of the brace to chord width ratio

Load-displacement curves and secondary bending stress with different β values are shown in Fig. 5, note that the points in Fig.5-b corresponds to the ultimate force. Joints with β2 and β3 obtained around 15%-18% and 34%-40% larger resistance when compared with joint with β1. The largest difference is obtained for joints with steel grade S355 and the lowest for joints with S960. For all the steel grades, with the increasing β value, the ultimate load resistance increases. However, the relative effect of the large β-value on high-strength joints, are lower compared to the joints with mild-strength steels. The maximum secondary bending moment for the models β1-S355 was $0.16fy$, β2-S355 is $0.19fy$ and β3-S355 was $0.23fy$. For the models β1-S960, β2-S960 and β3-S960 the maximum secondary bending moments are $0.22fy$, $0.26fy$ and $0.30fy$ respectively. The impact of larger β-value on the secondary bending stresses in high-strength joints is lower when compared to mild-strength steel.

3.5 Effects of weld types

The load-displacement curves with different weld types are plotted in Fig.6. The fillet-welded joints result in approximately 37% for S960, 28% for S700, 20% for S460 and 18% for S355

larger ultimate load resistance than in case of the butt-welded joints. This is due to the additional stiffness introduced by the fillet welds. The largest difference is obtained for the models with high strength steel S960. For each steel grade and for average stresses up to $0.2f_y$, a small difference in the secondary bending stress is observed. For average stress above $0.2f_y$, the secondary bending stresses for the fillet-welded joints are larger than for the butt-welded joints. This is due to the uneven stiffness distribution of the weld and the one-sided fillet welds.

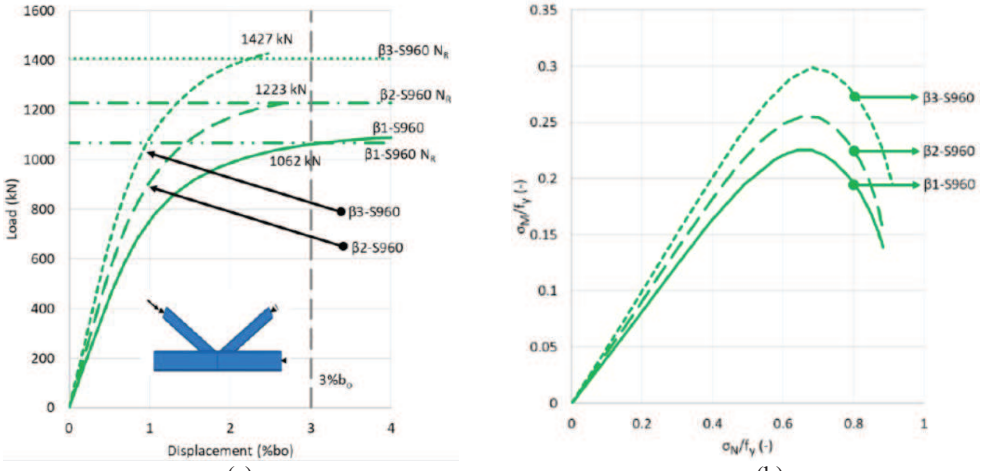

(a) (b)

Figure 5 Brace to chord width ratio effects (a) Load-displacement (b) The secondary bending stress

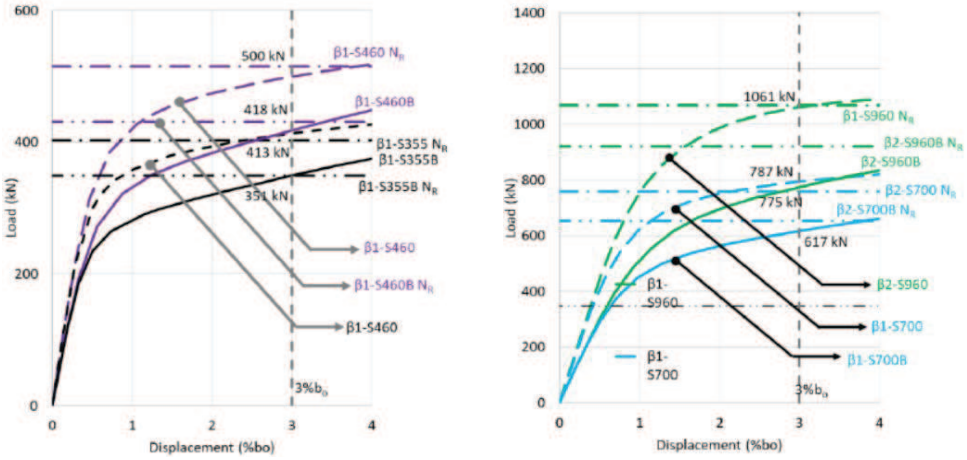

Figure 6. Load displacement relationship with different weld types

3.6 Yield line model

Deformation pattern of joint at ultimate load resistance are used to access the yield lines. As shown in Fig.7, yield lines are assumed to be straight and generally appear at the brace toe and heel. The length of the yield lines is measured using the tool "path". The external work is equal to the joint resistance multiplied by a small deflection of the chord face. The displaced, rotated yield lines and the plastic moment are used to determine the internal work.

The joint resistance is determined by dividing the internal work by the displacement of the chord face. As listed in Table 3, the joint resistance obtained by the yield line mechanism is 2%-16% lower compared to the ultimate load resistance obtained by the FEA.

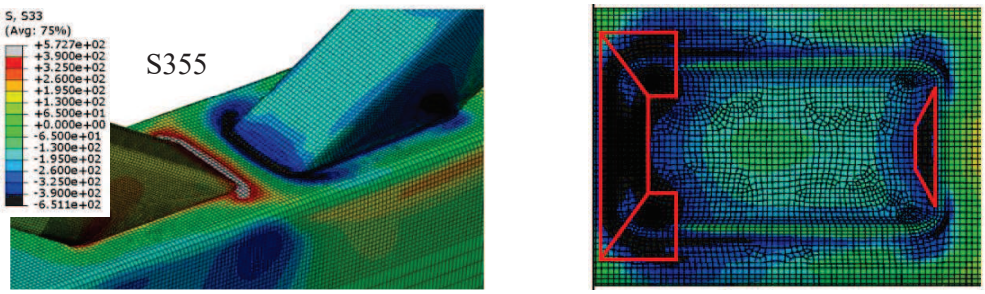

Figure 7. Yield line pattern of gap K-joints

Table 3. Resistance ratio between yield line methods and FE results (N_{YL}/N_{FEA})

Steel grade	K_3	K_4	K_6	K_7
S355	0.85	0.87	0.91	0.91
S460	0.92	0.88	0.91	0.86
S700	0.89	0.89	0.88	0.91
S960	0.88	0.84	0.88	0.98

3.6 Comparisons FE results and design proposals acc. a new version of EN1993-1-8

Fig.8 shows material reduction factor C_f distribution for various steel grades. EN1993-1-8-DRAFT V4.2 recommended that C_f=1.0 when $f_y \leq$ 355MPa, and C_f=0.9 when 355<$f_y \leq$ 460MPa, and C_f=0.8 when 460<$f_y \leq$ 700MPa. Based on the results presented in the paper, C_f is proposed as 1.0 when $f_y \leq$ 355MPa, 0.9 when 355<$f_y \leq$ 700MPa, and 0.8 when 700<$f_y \leq$ 960MPa. Note the assumption that material properties of welds and HAZ are same as the base material may affect the value of C_f. The values of reduction factor C_f need to be further improved.

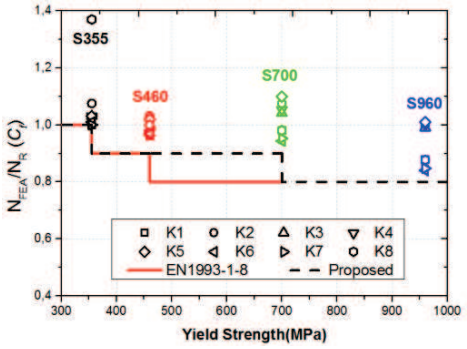

Figure 8. Material reduction factor C_f distribution along yield strength

4 CONCLUSIONS

A parametric study on the gap K joints is performed using "traditional" assumptions such as the same material properties for weld and base material and J2 plasticity model. Investigation of the material characteristics, gap size, the brace to chord width ratio and welds type effects on the secondary bending stresses were performed and following could be emphasized:

(1) K Joints with steel grade S460, S700, and S960 resulted in 20%, 83% and 142% larger ultimate load resistance compared to the joint with steel grade S355. The secondary bending moment is larger for joints with higher yield strengths steel grades. As the axial load increases the secondary bending stresses increases and decreases after the peak secondary bending stress has reached due to material softening. No decrease phase of secondary bending stress is observed from Bjork et al. 2015, which may be due to that the material damage is not considered. Note that the material models still need to be improved to better consider post necking behavior and multiaxial damage of the joints using HSS. These improvements may influence the ultimate resistance and failure mode. The material model used in this model underestimates the true stress magnitude after necking. After the onset of necking, the uniaxial stress status of coupon specimens are changed to complicated multiaxial stress see Ling 1996.

(2) The ultimate load resistance increases with increasing yield strength. Joints with lower gap size, exhibit larger secondary bending stresses and lower ratio between secondary bending stress to average axial stress than joint with larger gap size.

(3) For each steel grade, larger β-values result in larger secondary bending stresses. Influence of the larger β-values for higher strength hollow section joints are lower when compared to mild-strength hollow section joints. For each steel grade, the secondary bending stresses in the fillet-welded joints are larger than that of the butt-welded joints.

(4) Based on the results presented in the paper, C_f is proposed 1.0 when $f_y \leq 355$MPa, 0.9 when $355 < f_y \leq 700$MPa, and 0.8 when $700 < f_y \leq 960$MPa. Note that the material properties assumptions may affect the value of C_f. The values of reduction factor C_f will be further investigated by improved material models including distinction between HAZ, the filler material and base material.

References

Journal Papers

Bijlaard, F., Veljkovic, M., Shi, G., & Qiang, X. Editorial: Implementation of high-strength, high performance steel structures. Steel Construction, 11(4), 247-248, 2018.

Ling, Y. Uniaxial true stress-strain after necking. AMP Journal of technology, 5(1), 37-48, 1996.

Veljkovic, M., & Johansson, B. Design of hybrid steel girders. Journal of Constructional Steel Research, 60(3-5), 535-547, 2004.

Books

Wardenier, J., Packer, J. A., Zhao, X. L., & Van der Vegte, G. J. Hollow sections in structural applications. Rotterdam,, The Netherlands: Bouwen met staal. 2002.

Standardization, EN1993-1-8 v4.2 2018-07-27. Eurocode 3: Design of steel structures - Part 1-8: Design of joints.

Standardization, EN 1993-1-12. Eurocode 3: Design of steel structures - Part 1-12: Additional rules for the extension of EN 1993 up to steel grades S 700. 2011.

RUOSTE (2016). RUOSTE Project (Rules On High Strength Steel) RFSR-CT-2012-00036 - Final Report. Research Found For Coal and Steel.

Proceedings Papers

Bjork T., Tuominen N.P., Lahde T. Effect of the secondary bending moment on K-joint capacity. Proceedings of 14th International symposium on tubular structures. London, UK. 2015